Generalized Partial-Element Equivalent-Circuit Analysis for Planar Circuits With Slotted Ground

Kai Yang and Ke-Li Wu, *Senior Member, IEEE*

***Abstract*—A generalized partial-element equivalent-circuit (PEEC) method is proposed for modeling a planar circuit with a thin narrow slot on the ground. The approach is based on the coupled mixed potential integral equations for a problem with mixed electric and magnetic currents. The coupled integral equations are converted into a lumped-element circuit network using Kirchhoff's voltage law and Kirchhoff's current law of the circuit theory. The full-wave Green's functions for a grounded dielectric substrate problem are used. The interactions between electric current on a microstrip line and magnetic current on a slot are taken into account by introducing two kinds of controlled sources. This generalized PEEC model will be very useful in signal-integrity analysis for multilayered circuits. To validate the generalized model, three numerical examples consisting of microstrip lines and slots on the ground are presented. The results obtained by the proposed generalized PEEC model are compared with those obtained by commercial electromagnetic simulation software and published experimental results. Good agreement is obtained.**

***Index Terms*—Green's functions, mixed potential integral equation (MPIE), partial element equivalent circuit (PEEC), planar circuits, slotted ground.**

I. Introduction

THE partial-element equivalent-circuit (PEEC) [1] model, which is based on the electric field mixed potential integral equation (EF-MPIE), has been widely used for electromagnetic (EM) modeling of various engineering problems [2]–[4] including electromagnetic compatibility (EMC), electromagnetic interference (EMI), and signal integrity (SI) of high-speed digital circuits. The main advantage of the PEEC model, as compared to other integral-equation-based EM modeling methodologies, such as the method of moments (MOM), is that it can convert a physical circuit layout into a mesh related lumped-element circuit network. The network can then be easily analyzed using a general-purpose circuit simulator, such as SPICE, both in the frequency and time domains. This feature makes the model very attractive to researchers who are interested in system-level mixed-signal simulations on an integrated cross-disciplinary simulation platform. Therefore, the development and applications of the PEEC have never been stopped. For example, the PEEC was used to analyze spiral inductors and transformers in RF integrated circuits (RFICs) [5] and was also employed for modeling multichip modules [6]. Recently, Wang and Wu [7] have proposed a derived physically expressive circuit (DPEC) method, which can turn a PEEC network into a concise and physically meaningful circuit model, for analyzing multilayered RF embedded passives. The DPEC algorithm can reduce the order of a PEEC model by a few orders of magnitude so that the resultant concise circuit model can be easily analyzed or physically understood. More recently, the DPEC model has been extended to lossy RF passive circuits and has been successfully used to derive the physically meaningful circuit models of multilayer on-chip inductors [8]. In conjunction with the DPEC model, the PEEC model will find more and more applications in the modeling of electrically large problems and will provide circuit designers with a physical insight into a circuit layout. Therefore, enhancing the capability and improving the performance of the PEEC model will raise great interests in the industry. One of the immediately needed extensions of the traditional PEEC model is the inclusion of the magnetic current and the couplings between the electric current and the magnetic current. Needless to say, the most prominent magnetic current problem is a multilayer circuit with a slotted infinitely large ground plane.

Although several PEEC-based commercial EM software tools have emerged in recent years,[1,2] to the best of our knowledge, there are few PEEC models [9], [10] that can handle the magnetic current problem, especially for the slotted ground structures. The conventional PEEC is difficult to analyze a planar circuit with slotted ground unless the ground plane is also discretized by meshes to the farthest extent of computational limit, which makes the traditional PEEC method highly computationally expensive and impractical. Introducing an equivalent magnetic current to replace a slot removes the need of meshing the ground plane, and therefore, significantly improves the efficiency of the PEEC model in handling a high layer count multilayered circuit problem.

Aperture-coupled microstrip lines and microstrip circuits with defected ground are typical slotted ground problems. The problems have drawn a great deal of attention due to their high-impedance properties for certain frequency bands [11], better isolation, and common mode rejection properties if the slot pattern is appropriately designed [12]. Pozar [13] utilized the MOM together with the reciprocity theorem to investigate a thin slot in the ground plane and its coupling with an infinitely long microstrip line. Later, Kahrizi *et al.* [14] analyzed a wide radiating slot. In [15], Sercu *et al.* employed mixed rectangular and triangular meshes for modeling hybrid microstrip-slotline

Manuscript received November 29, 2008; revised March 02, 2009. First published May 27, 2009; current version published July 09, 2009. This work was supported by the Research Grants Council of the Hong Kong Special Administrative Region under Grant 417006.

The authors are with the Department of Electronic Engineering, The Chinese University of Hong Kong, Shatin, Hong Kong (e-mail: klwu@ee.cuhk.edu.hk).

Color versions of one or more of the figures in this paper are available online at http://ieeexplore.ieee.org.

Digital Object Identifier 10.1109/TMTT.2009.2022589

[1]Advanced EMC Solutions, Winnipeg, MB, Canada. [Online]. Available: http://www.aemcs.com/statmod.html

[2]Ansoft, Pittsburgh, PA. [Online]. Available: http://www.ansoft.com/products/si/tpa

multilayered circuits. The sub-sectional basis function has been utilized to investigate an arbitrarily shaped aperture-coupled patch antenna in [16]. Most of these works studied the problem from the viewpoint of the MOM with the coupled electric field and magnetic field mixed potential integral equations (MPIEs), and accurately predicted the performance of the slotted ground structures by their S-parameters. However, these MoM-based models cannot lead to a lumped-element circuit model that physically maps to a circuit structure, and such a circuit model is highly desirable.

In this paper, an extension of the traditional PEEC model is proposed for modeling a planar circuit with slotted ground. Since this extended PEEC has incorporated all the possible field couplings generated by electric and magnetic currents, the formulation is considered as the most general PEEC model for a multilayer circuit. This work is the first attempt that converts a multilayer circuit with slotted ground into a lumped circuit model through the coupled MPIE. The circuit model generated by the proposed theory provides a full-wave equivalent-circuit representation to a multilayered circuit with slotted ground. This generalized PEEC model makes it possible to integrate a multilayer circuit seamlessly with SPICE-like circuit simulator and enables the PEEC method to be a very powerful modeling methodology.

In the proposed analysis, magnetic current is used to represent the tangential electric field on the slot. A pulse basis function is used to expand the electric current, magnetic current, and the corresponding electric and magnetic charges on the microstrip and slot structures, respectively. The spectral-domain Green's functions given in [17] are used and the discrete image theory proposed in [18] is utilized for obtaining the Green's functions in the spatial domain.

This paper is organized as follows. The basic theory is presented in Section II, where Kirchhoff's voltage law (KVL) and Kirchhoff's current law (KCL) are used to interpret the coupled MPIEs in terms of circuit domain language. In Section III, three representative examples are numerically analyzed and modeled by the proposed method. The numerical results are compared with commercial EM software simulation and published measurement data. Section IV presents discussions and a conclusion.

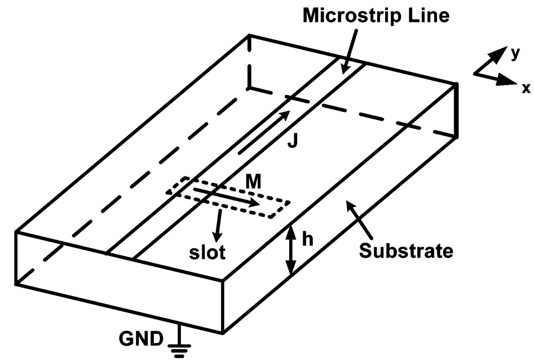

(a)

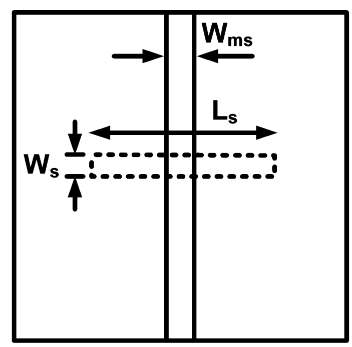

(b)

Fig. 1. Configuration of a slotted ground microstrip. (a) 3-D view. (b) Top view.

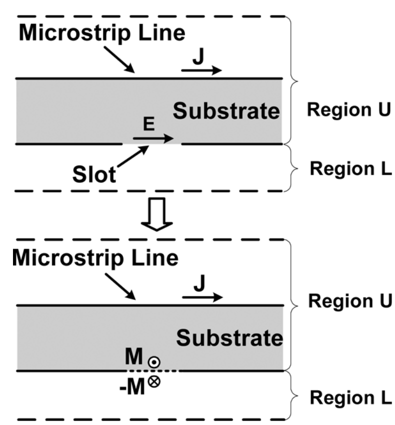

Fig. 2. Application of the equivalence principle.

II. Theory

The geometry of a typical slotted ground problem is shown in Fig. 1. The ground plane coincides with the $z = 0$ plane, and the thickness of the microstrip substrate is h. The ground plane and dielectric layer are assumed to be perpendicular to the $\vec{z}$-axis and extend to infinity in the x- and y-directions. The electric current $\vec{J}$ on the microstrip line is y-directed. The electric field across the slot is assumed to have only a y-directed component in a narrow slot case. This assumption does not lose any generality. Under the assumption of a thin slot, the slot can be closed up and be replaced by an equivalent magnetic current sheet of $\pm\vec{M}$ according to the equivalence principle illustrated in Fig. 2.

The original problem can now be separated into two independent problems. Above the ground plane $(z > 0)$, the equivalent problem has the electric current $\vec{J}$ at the microstrip line and the magnetic current $\vec{M}$ at $z = 0^+$ just above the closed slot. Below the ground plane $(z < 0)$, the equivalent problem has only the magnetic current $-\vec{M}$ at $z = 0^-$ just below the closed slot. From the equivalence principle, it is known that

$$\vec{M} = \vec{E} \times \hat{z}. \quad (1)$$

The two sub-problems are connected by enforcing the boundary conditions on the slot, where the tangential electric and magnetic fields are continuous.

A. MPIEs

Considering the boundary conditions on the microstrip line and the slot, one can easily find the following set of equations for $\vec{J}$ and $\vec{M}$:

$$\hat{z} \times [\vec{E}(\vec{J}) + \vec{E}(\vec{M})]_{\text{microstrip}} = 0 \quad (2)$$

$$\hat{z} \times [\vec{H}(\vec{J}) + \vec{H}(\vec{M}) + \vec{H}(-\vec{M})]_{\text{slot}} = 0 \quad (3)$$

where $\vec{E}(\vec{J})$ and $\vec{H}(\vec{J})$ are the electric and magnetic fields due to the electric current at the microstrip line, respectively, and $\vec{E}(\vec{M})$ and $\vec{H}(\pm\vec{M})$ are the electric and magnetic fields due to the magnetic current in the slot, respectively. The electric and magnetic fields can be expressed by vector and scalar potential functions as

$$\vec{E}(\vec{J}) = -j\omega\vec{A} - \nabla\phi \quad (4)$$

$$\vec{H}(\vec{M}) = -j\omega\vec{F}_U - \nabla\phi_U^M \quad (5)$$

$$\vec{H}(-\vec{M}) = -j\omega\vec{F}_L - \nabla\phi_L^M \quad (6)$$

where $\vec{A}, \vec{F}_U, \vec{F}_L, \phi, \phi_U^M, \phi_L^M$ are vector and scalar potentials from the electric and magnetic sources, respectively, in which subscripts U and L refer to the potentials generated from the magnetic sources above the slot and below the slot, respectively. Substituting (4)–(6) into (2) and (3) leads to

$$z \times \left[-\frac{\vec{J}}{\sigma} - j\omega\vec{A} - \nabla\phi + \vec{E}(\vec{M})\right]_{\text{microstrip}} = 0 \quad (7)$$

$$z \times \left[\vec{H}(\vec{J}) - j\omega\vec{F}_U - \nabla\phi_U^M - j\omega\vec{F}_L - \nabla\phi_L^M\right]_{\text{slot}} = 0. \quad (8)$$

For the convenience of the following deduction, the mixed fields of $\vec{E}(\vec{M})$ and $\vec{H}(\vec{J})$ are still represented by the abstract notations for now. All the potential functions and fields are expressed in terms of their Green's functions. Specifically,

$$\vec{A} = \int_{S_{\text{microstrip}}} \overline{\overline{G^A}} \cdot \vec{J} ds \quad (9a)$$

$$\phi = \int_{S_{\text{microstrip}}} G^q q ds \quad (9b)$$

$$\vec{E}(\vec{M}) = \int_{S_{\text{slot}}} \overline{\overline{G^{\text{EM}}}} \cdot \vec{M} ds \quad (9c)$$

$$\vec{H}(\vec{J}) = \int_{S_{\text{microstrip}}} \overline{\overline{G^{HJ}}} \cdot \vec{J} ds \quad (9d)$$

$$\vec{F}_U = \int_{S_{\text{slot}}} \overline{\overline{G_U^F}} \cdot \vec{M} ds \quad (9e)$$

$$\vec{F}_L = \int_{S_{\text{slot}}} \overline{\overline{G_L^F}} \cdot (-\vec{M}) ds \quad (9f)$$

$$\phi_U^M = \int_{S_{\text{slot}}} G_U^{q_M} q^M ds \quad (9g)$$

$$\phi_L^M = \int_{S_{\text{slot}}} G_L^{q_M} (-q^M) ds \quad (9h)$$

where $\overline{\overline{G^A}}, G^q, \overline{\overline{G_U^F}}, \overline{\overline{G_L^F}}, G_U^{q_M}, G_L^{q_M}, \overline{\overline{G^{\text{EM}}}}$, and $\overline{\overline{G^{HJ}}}$ are spatial-domain dyadic Green's functions of vector and scale potentials and electric and magnetic fields generated by electric and magnetic sources. The dyadic potential Green's functions are first derived by employing a transmission line network analog of the multilayer medium [17] in the spectral domain. The discrete complex image method (DCIM) [18] is then applied to accelerate the evaluation of the Sommerfeld integration in calculating the spatial Green's functions at a different frequency. q and q^M are the electric and magnetic charge densities, which are related to $\vec{J}$ and $\vec{M}$ by the current continuity laws.

In Fig. 1, it is assumed that the electrical current at the microstrip line only has a y component $\hat{y}J_y$, whereas the magnetic current on the slot only has an x component $\hat{x}M_x$ above the slot and $-\hat{x}M_x$ below the slot. Like the traditional PEEC model, all the electric and magnetic sources in (9) are expanded by the pulse basis functions. Namely,

$$J_y(r') = \sum_{i=1}^{M_1} J_{yi} p_i(r') \quad (10a)$$

$$q(r') = \sum_{j=1}^{N_1} q_j p_j(r') \quad (10b)$$

$$M_x(r') = \sum_{k=1}^{M_2} M_{xk} p_k(r') \quad (10c)$$

$$q^M(r') = \sum_{l=1}^{N_2} q_l^M p_l(r') \quad (10d)$$

where

$$p_n(r') = \begin{cases} 1, & r' \in n\text{th cell of current or charge} \\ 0, & r' \in \text{else where} \end{cases} \quad (10e)$$

and M_1, M_2 and N_1, N_2 are the number of basis functions used to descretize the density functions of the electric current, magnetic current, electric charge, and magnetic charge, respectively. For the simplicity, the source position variable r' will be omitted in the following equations. Substituting the expressions in (10) into (7)–(9h) results in the following equations:

$$\begin{aligned} &\sum_{i=1}^{M_1} \frac{J_{yi}}{\sigma} + j\omega \sum_{i=1}^{M_1} \int_{S_{\text{microstrip}}} G_{yy}^A J_{yi} ds \\ &\quad + \sum_{j=1}^{N_1} \frac{\partial}{\partial y} \int_{S_{\text{microstrip}}} G^q q_j ds \\ &\quad - \sum_{k=1}^{M_2} \int_{S_{\text{slot}}} G_{yx}^{\text{EM}} M_{xk} ds \\ &= 0 \end{aligned} \quad (11)$$

$$\begin{aligned} &j\omega \sum_{k=1}^{M_2} \int_{S_{\text{slot}}} G_{U+L}^M|_{xx} M_{xk} ds \\ &\quad + \sum_{l=1}^{N_2} \frac{\partial}{\partial x} \int_{S_{\text{slot}}} G_{U+L}^q q_l^M ds \\ &\quad - \sum_{i=1}^{M_1} \int_{S_{\text{microstrip}}} G_{xy}^{HJ} J_{yi} ds \\ &= 0 \end{aligned} \quad (12)$$

where

$$G_{U+L}^M = G_U^M + G_L^M \quad (13)$$

and

$$G_{U+L}^{q_M} = G_U^{q_M} + G_L^{q_M}. \quad (14)$$

The electric and magnetic current densities in (11) and (12) can be written in terms of the electric and magnetic currents. One set of coupled equations are obtained by the integration of (11) over all surface cells of the microstrip line. Integrating (11) over the mth cell of the microstrip line and dividing the equation by the transversal width of the cell a_m leads to

$$\begin{aligned}&\sum_{i=1}^{M_1}\frac{1}{a_i a_m}\int_{S_m}\frac{I_{yi}}{\sigma}ds+j\omega\sum_{i=1}^{M_1}\frac{1}{a_i a_m}\\&\quad\times\int_{S_m}\int_{S_i}G_{yy}^{A}I_{yi}ds ds\\&\quad+\sum_{j=1}^{N_1}\frac{1}{a_m}\int_{S_m}\frac{\partial}{\partial y}\int_{S_j}G^{q}q_j ds\,ds\\&\quad+\sum_{k=1}^{M_2}\frac{1}{a_k a_m}\int_{S_t}\int_{S_k}\left(-G_{yx}^{\mathrm{EM}}\right)I_{xk}^{M}ds\,ds=0.\end{aligned}\tag{15}$$

Here, $S_i, S_m S_j$, and S_k represents the electric current cell i, the electric current cell m, electric charge cell j, and magnetic current cell k, respectively, and $m=1,2,\ldots,M_1$.

The other set of coupled equations are obtained by the integration of (12) over all the magnetic current cells on the slot. Particularly, integrating (12) over the nth cell on the slot and dividing the equation by the transversal width of the cell $a_n (n=1,2,\ldots,M_2)$ leads to

$$\begin{aligned}&j\omega\sum_{k=1}^{M_2}\frac{1}{a_k a_n}\int_{S_n}\int_{S_k}G_{U+L}^{M}|_{xx}I_{xk}^{M}ds\,ds\\&\quad+\sum_{l=1}^{N_2}\frac{1}{a_n}\int_{S_n}\frac{\partial}{\partial x}\int_{S_l}G_{U+L}^{q_M}|_{xx}q_l^{M}ds ds\\&\quad+\sum_{i=1}^{M_1}\frac{1}{a_i a_n}\int_{S_n}\int_{S_l}\left(-G_{xy}^{HJ}\right)I_{yi}ds\,ds=0.\end{aligned}\tag{16}$$

In order to better understand the coupled integral equations from the circuit theory point of view, the electric and magnetic current densities in (15) and (16) are expressed by their corresponding currents divided by the transverse widths of the electric current cell a_{L_1} and the magnetic current cell a_{L_2}, respectively. In fact, (15) can be interpreted as a voltage loop equation $V_R+V_L+V_C+V_{\mathrm{VCVS}}=0$ using KVL and (16) can be interpreted as a current node equation $I_C+I_L+I_{\mathrm{CCCS}}=0$ from the KCL point of view. Fig. 3 illustrates the circuit interpretations for a typical electric current cell and a typical magnetic current cell. It is interesting to see that the duality between the circuits in Fig. 3(a) and (b) also follows the basic relationship between the electric current/charge and magnetic current/charge.

B. Meshing Scheme and Circuit Interpretation

Before introducing the circuit interpretation, we first define four types of cell including the electric current cells, electric charge cells, magnetic current cells, and magnetic charge cells in the mesh scheme. Fig. 4 illustrates the meshing scheme, in which solid lines are used to represent the electric and magnetic current cells, while the dashed lines are for electric and magnetic charge cells. The electric current cells are shifted by half the size of the corresponding electric charge cells, as described in [1], whereas the magnetic charge cells are shifted by half the size of the corresponding magnetic current cells in the same way as that used in electric cell meshing. The four kinds of cells are modeled by inductive and capacitive elements that are to be explained later. The mutual couplings between different types of source will be viewed as controlled sources.

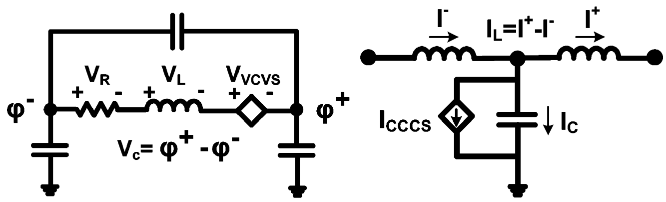

(a) (b)

Fig. 3. Circuit representation of the discretized MPIE. (a) Electric current cell. (b) Magnetic current cell.

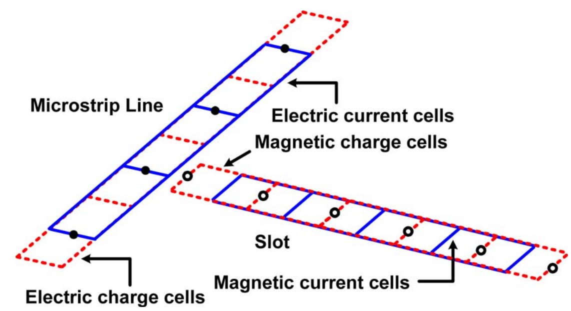

Fig. 4. Discretization of a microstrip line with a slotted ground.

In order to convert a multilayer circuit layout with a slotted ground into a PEEC model, the conduct traces (in this case, the microstrip line), as well as the slot on the ground need to be meshed first. In Fig. 4, the solid dots represent the network nodes of the electric charges at a microstrip line, whereas the hollow dots represent the nodes of the magnetic charges on the slot. The electric current cells at the microstrip line and magnetic current cells on the slot are represented by solid rectangles. Similarly, the electric charge cells at a microstrip line and the magnetic charge cells at a slot are represented by dotted rectangles.

The concept of the complex inductor and capacitor introduced in [8] will be utilized in this work in order to incorporate various loss mechanisms. In addition, all lumped elements in the PEEC model have frequency-dependent complex values. The physical meanings of the first three terms in (15) have been explained in [1]. For the completeness of the discussion, they are repeated here. Namely, they represent the resistive, inductive and capacitive contributions to the voltage loop equation defined by a basic electric current cell, respectively, and can be expressed by

$$V_R=R_m I_{ym}$$

where

$$R_m=\frac{1}{a_i a_m}\int_{S_m}\frac{1}{\sigma}ds,\qquad i=m\tag{17}$$

$$V_L=\sum_{i=1}^{M_1}j\omega L_{i,m}I_{yi}$$

where

$$L_{i,m} = \frac{1}{a_i a_m} \int_{S_m} \int_{S_i} G_{yy}^A ds ds \tag{18}$$

and

$$\begin{aligned} V_C &= \sum_{j=1}^{N_i} \frac{q_j}{a_m} \left(\int_{S_m} \frac{\partial}{\partial y} \int_{S_j} G^q ds ds \right) \\ &= \sum_{j=1}^{N_i} \frac{Q_j}{a_m S_j} \left(\int_{S_m} \frac{\partial}{\partial y} \int_{S_j} G^q ds ds \right) \\ &= \sum_{j=1}^{N_i} \frac{Q_j}{S_j} \left(\int_{S_j} G^q(r_j^+, r') ds - \int_{S_j} G^q(r_j^-, r') ds \right) \\ &= \varphi^+ - \varphi^- \end{aligned} \tag{19}$$

respectively.

The fourth term of (15), which is not included in the traditional PEEC model and is rewritten here for clarity, is introduced by the magnetic current on the slot

$$V_{\text{VCVS}} = \sum_{k=1}^{M_2} \left\{ \frac{1}{a_k a_m} \int_{S_m} \int_{S_k} \left(-G_{yx}^{\text{EM}} \right) ds ds \right\} I_{xk}^M. \tag{20}$$

Since the unit dimension of the magnetic current is in volt, this term can be interpreted as a voltage-controlled voltage source (VCVS). Consequently, a magnetic current cell can be viewed as a voltage source in the circuit domain. The term in the curly brackets is an integration of the normalized electric field generated by a magnetic current cell k over electric current cell m and can be recognized as the voltage gain coefficient μ_{mk} of a VCVS at an electric current cell m, in which the controlling voltage source is the kth magnetic current cell on the slot. Clearly, a VCVS represents the summed voltage on an electric current cell m contributed by all the magnetic current cells. Concisely, it can be expressed as

$$V_{\text{VCVS}} = \sum_{k=1}^{M_2} \mu_{m,k} I_{xk}^M. \tag{21}$$

The magnetic field continuity equation (16) reveals the current continuity from the circuit theory point of view and has not been included in the traditional PEEC model. The three terms in (16) represents different branch current shown in Fig. 3(b). The first term in (16) that represents a capacitive coupling is rewritten here for clarity as follows:

$$I_C = \sum_{k=1}^{M_2} j\omega \left\{ \frac{1}{a_k a_n} \int_{S_n} \int_{S_k} G_{U+L}^M|_{xx} ds ds \right\} I_{xk}^M. \tag{22}$$

I_C is the current flow through the capacitor in Fig. 3(b). The term in the curly brackets is recognized as the capacitances. The summation in (22) represents the coupling among them. In other words,

$$I_C = \sum_{k=1}^{M_2} j\omega C_{k,n}^{SC} I_{xk}^M, \qquad n = 1, 2, \ldots, M_2. \tag{23}$$

The coefficients $C_{k,n}^{SC}$ then construct the short-circuit capacitance matrix, which is related to the capacitances in the equivalent circuit with M_2 nodes by [19]

$$C_{i,i} = \sum_{j=1}^{M_2} C_{i,j}^{CS}, \qquad i = 1, 2, \ldots, M_2 \tag{24a}$$

$$C_{i,j} = -C_{i,j}^{SC}, \qquad i \neq j \tag{24b}$$

where $C_{i,i}$ and $C_{i,j}$ are the self-capacitance at node i and mutual capacitance between node i and node j, respectively.

The second term in (16) is related to the inductive contribution to the PEEC sub-circuit directly associated to the slot. Using the approximation that

$$\int_{S_n} \frac{\partial}{\partial x} F(x, y, z, x', y', z') ds \approx a_n [F(x^+ y, z, x', y', z') - F(x^- y, z, x', y', z')] \tag{25}$$

the second term in (16) can be expressed as

$$I_L = \sum_{l=1}^{N_2} \frac{Q_l^M}{S_l} \left\{ \int_{S_l} G_{U+L}^{q_M}(x^+, y, z, x', y', z') - G_{U+L}^{q_M}(x^-, y, z, x', y', z') ds \right\} \tag{26}$$

where Q_l^M is the total magnetic charge over magnetic charge cell l. Note that the magnetic charge density q_l^M in (16) is expressed by Q_l^M / S_l. Here, S_n and S_l are the areas of magnetic current cell n and magnetic charge cell l on the slot, respectively. Be noted that a magnetic charge cell is obtained by shifting its corresponding magnetic current cell by half the cell size.

It is clear that the current I_L is the linear superposition of all the contributions by the magnetic charges over N_2 magnetic charge cells on the slot, or

$$I_L = \sum_{l=1}^{N_2} Q_l^M \left[ff_{l,n}^+ - ff_{l,n}^- \right] = I^+ - I^- \tag{27}$$

where $[ff_{l,n}^+ - ff_{l,n}^-]$ defines the matrix of *coefficients of magnetic potential*. Considering the relation between a magnetic current and a magnetic charge that

$$Q^M = \frac{I^M}{j\omega} \tag{28}$$

one can find

$$I_L = \sum_{l=1}^{N_2} \frac{I_l^M}{j\omega} [ff_{l,n}^+ - ff_{l,n}^-] = I^+ - I^-, \quad n = 1, 2, \ldots, N_2. \tag{29}$$

That is to say, I_L is the difference between the currents flow through the two inductors, as shown in Fig. 3(b). It is interesting to see that the unit dimension of ff^+, ff^- is reciprocal of inductance. Therefore, the inverse of the matrix $[ff_{l,n}^+ - ff_{l,n}^-]$ can be interpreted as an inductance matrix in accordance with the

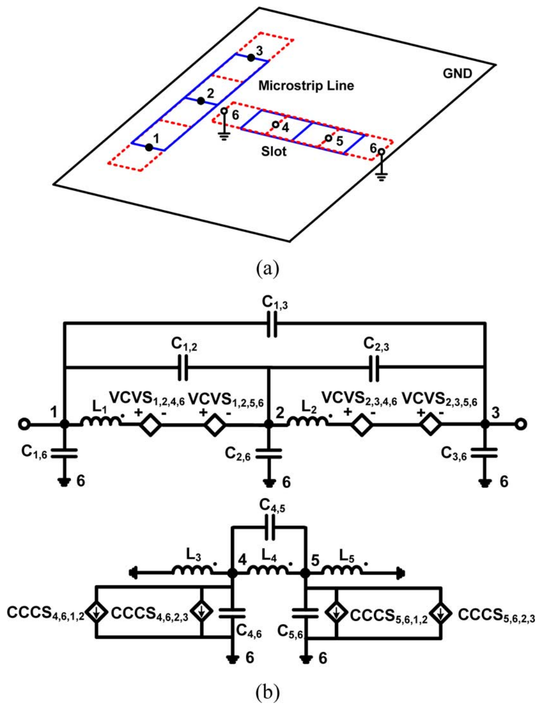

Fig. 5. Generalized PEEC model of a slotted ground microstrip. (a) Meshes of the slotted ground microstrip. (b) Equivalent circuit.

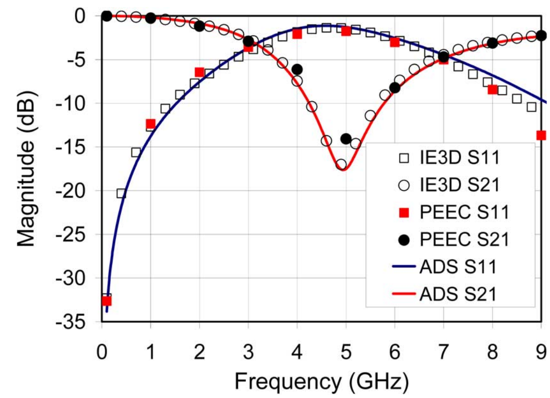

Fig. 6. Comparison of S-parameters obtained by the generalized PEEC model, IE3D and ADS.

conventional definition in circuit theory. Having had the inductance matrix defined, one can construct a full network of partial inductances for all magnetic charge cells.

Similar to the VCVS in (20), the third term in (16) can be viewed as a current-controlled current source (CCCS) from circuit theory point of view

$$I_{\rm CCCS} = \sum_{i=1}^{M_1} \left\{ \frac{1}{a_i a_n} \int_{S_n} \int_{S_i} \left(-G_{xy}^{HJ}\right) ds ds \right\} I_{yi}. \quad (30)$$

$I_{\rm CCCS}$ is the current flow through the CCCS in Fig. 3(b). The term in the curly brackets is defined as a complex current gain coefficient α_{ni} at magnetic current cell n. The controlling current source is the electric current at current cell i. The CCCS represents the magnetic field on the slot generated by the electric current at the microstrip line. In a compact form, (30) can be expressed as

$$I_{\rm CCCS} = \sum_{i=1}^{M_1} \alpha_{n,i} I_{yi}. \quad (31)$$

Until now, every field related term in the coupled MPIEs has been explained by its counterpart in the circuit domain. A complex valued network representation of a planar circuit with slotted ground can be obtained by the proposed generalized PEEC model.

To illustrate the generalized PEEC model, Fig. 5 shows the PEEC model of a slotted ground microstrip with a simple mesh illustration, in which there are two electric current cells and three electric charge cells on the microstrip line and two magnetic current cells and three magnetic charge cells on the slot. In Fig. 5(b), all the mutual inductances and mutual capacitances are suppressed for clarity. Note that there are no mutual inductances and capacitances between the cells on the microstrip and those on the slot. The couplings between the microstrip line and slot are presented through two types of controlled source. The VCVS models the influence of the magnetic current on the slot to the voltage at the microstrip line, whereas CCCS represents the additional electric current across the slot. The controlled voltages $\mathrm{VCVS}_{1,2,4,6}$ and $\mathrm{VCVS}_{2,3,4,6}$ are controlled by the voltage between nodes 4 and 6, whereas $\mathrm{VCVS}_{1,2,5,6}$, and $\mathrm{VCVS}_{2,3,5,6}$ are controlled by the voltage between nodes 5 and 6. $\mathrm{CCCS}_{4,6,1,2}$ and $\mathrm{CCCS}_{5,6,1,2}$ are controlled by the current flowing through $L_{1,2}$, and $\mathrm{CCCS}_{4,6,2,3}$ and $\mathrm{CCCS}_{5,6,2,3}$ are controlled by the current flowing through $L_{2,3}$.

III. Numerical Examples

To validate the generalized PEEC model, three numerical examples are investigated. The first numerical example is a typical slotted ground microstrip line shown in Fig. 1. The geometry of the narrow slot is $L_s = 26$ mm and $W_s = 1$ mm. The microstrip line is 30-mm long with the width $W_{\rm ms} = 2$ mm. The substrate is with the thickness $h = 0.7$ mm and the relative permittivity $\varepsilon_r = 2.5$. In the frequency range of interest, it is assumed that the characteristic impedance of the microstrip line is 50 Ω. The microstrip is divided into 26 cells and the slot is divided into 30 cells. The generalized PEEC model generated by the formula discussed above contains more than 1600 circuit elements. Once the PEEC circuit model is generated using the theory presented, an in-house circuit simulator is used to analyze the network and to generate the S-parameters. Fig. 6 shows the magnitude of the S-parameters generated by the generalized PEEC model, commercial EM simulation software IE3D [20], and ADS [21]. Good agreement is observed.

The second example is a microstrip line with two thin slots on the ground, as depicted in Fig. 7. The geometry of the narrow slots is $L_s = 20$ mm and $W_s = 1$ mm. The microstrip line is 40-mm long with the width $W_{\rm ms} = 2$ mm. The separation distance between two slots is $d = 5$ mm. The substrate is with thickness $h = 0.7$ mm and the relative permittivity $\varepsilon_r = 2.5$. The microstrip is divided into 20 cells and the slot is divided into 40 cells. The PEEC model generated consists of more than 3200

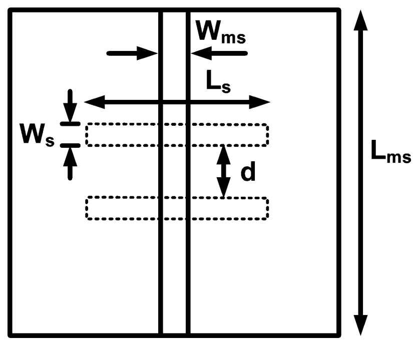

Fig. 7. Configuration of a double-slotted ground microstrip.

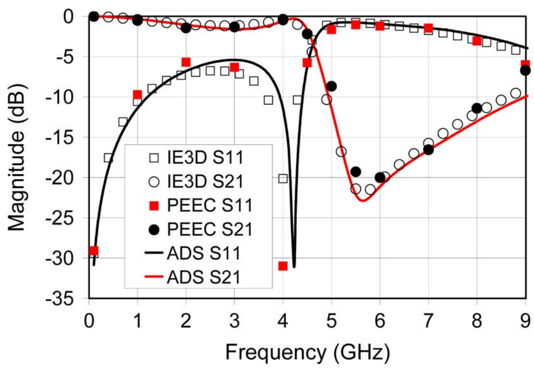

Fig. 8. Comparison of S-parameters obtained by the generalized PEEC model and EM simulation.

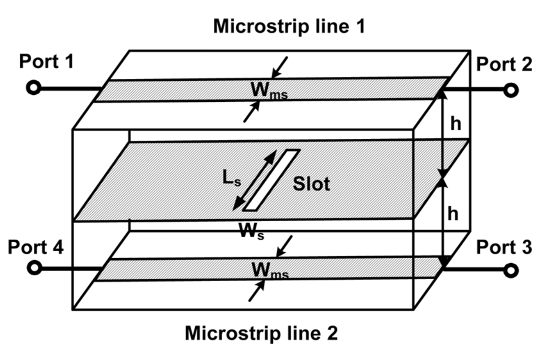

Fig. 9. Geometry of the slot-coupled microstrip lines.

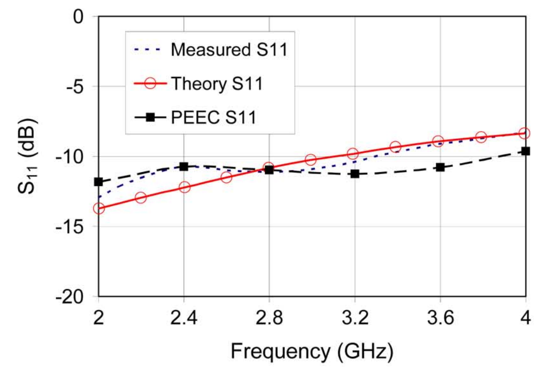

(a)

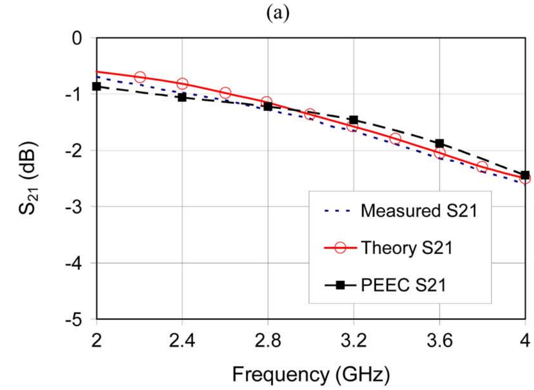

(b)

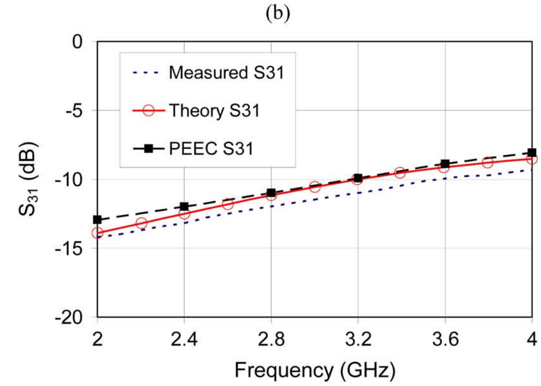

(c)

Fig. 10. Comparison of S-parameters obtained by the generalized PEEC model, theoretic and experimental results. (a) S_{11}. (b) S_{21}. (c) S_{31}.

circuit elements. Fig. 8 shows the comparison of the S-parameters calculated by the generalized PEEC mode, commercial software IE3D [20], and ADS [21]. Again, good agreement among them is obtained.

To show the potential application of the generalized PEEC model to a multilayer interconnection problem, the case of two parallel microstrip lines coupled through a thin narrow slot in the common ground plane is investigated as the last numerical example. This structure, which is shown in Fig. 9, has been studied in [15] and [22] using the MOM and reciprocity theorem.

The geometric parameters of the slot-coupled microstrip lines are $W_{\rm ms} = 2.54$ mm, $L_s = 15$ mm, $W_s = 1.1$ mm, $h = 0.762$ mm, and $\varepsilon_r = 2.22$. In this example, the generalized PEEC model consists of three blocks: two blocks are associated to the two microstrip lines and one block is associated to the slot. The two microstrip line related blocks are connected via the slot related block through the VCVSs and CCCSs. The microstrip is divided into 30 cells and the slot is divided into 15 cells. The final PEEC network consists of more than 1900 circuit elements. The calculated S-parameter using the proposed PEEC model is superposed with those from the reciprocity theory and the published measurement results [22] in Fig. 10. Fig. 11 illustrates a small part of the final PEEC model because of limited page space.

It has been demonstrated through the above three examples that the circuit networks generated using the proposed generalized PEEC model can very well reveal the physical phenomena of the original problems in a wide range of frequency. For the circuit simulation of above PEEC networks, an efficient in-house circuit simulator, which is based on the admittance node analysis, is used.

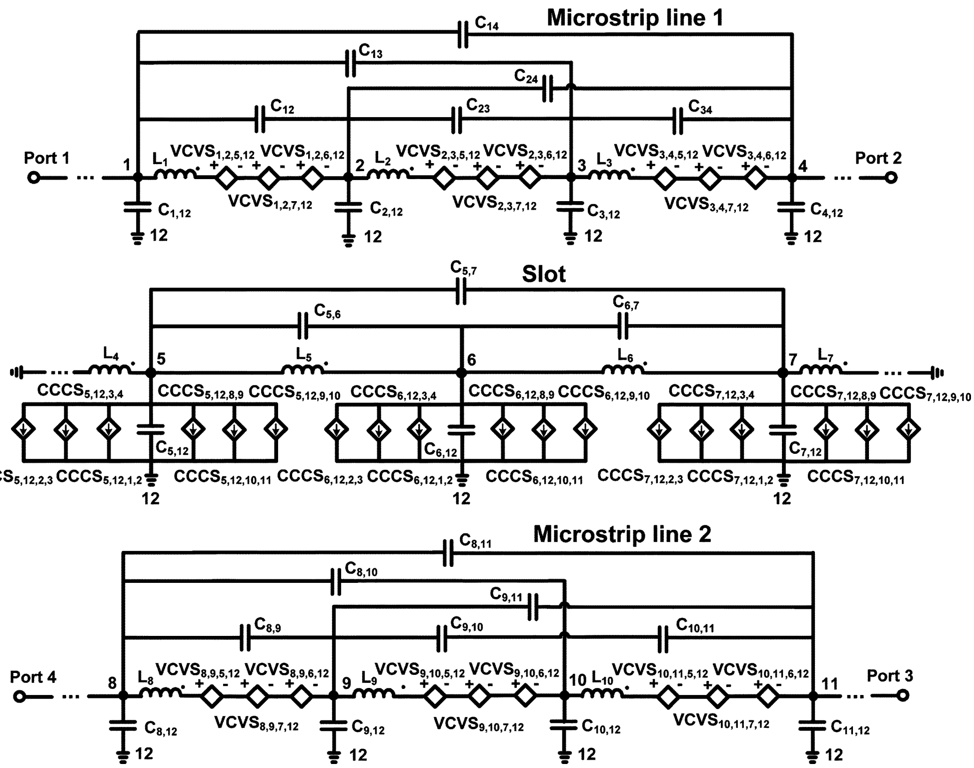

Fig. 11. Partial generalized PEEC model of the slot-coupled microstrip lines.

IV. Conclusion and Discussions

In this paper, a new generalized PEEC scheme for modeling a slotted ground structure has been proposed. This work is a substantial extension of the original PEEC model. By introducing the magnetic current and charge cells at the slot on the ground, the PEEC modeling of the EM problem with defected ground is greatly facilitated. Since the generalized PEEC method converts a multilayer physical layout containing multilayer conductor traces and a ground plane with coupling slots, into a circuit network, which is described by lumped circuit elements. The model can be useful to the applications where a circuit representation is much more desirable than scattering parameters in a frequency range. Three representative examples are given to demonstrate the effectiveness and validity of the proposed method.

The basic concept and theory of this model can be used to find more specific PEEC models for some *ad hoc* coupling structures on the ground plane, such as the ground with via-holes and apertures of arbitrary shapes. By applying the DPEC technique to this generalized PEEC model, people can derive the physically meaningful circuit models for any functional composite circuit elements such as planar metamaterial structures and to reveal their working mechanism in a plain circuit domain language.

It is worth mentioning that there are still many unsolved issues in PEEC modeling, and not enough attention have been paid to this useful approach from the computational electromagnetics community. In this work, the main focus is placed on the EM energy transmission problems in which insignificant energy radiates. For radiation problems, the radiation fields need to be extracted from the full wave Green's functions in the treatment of the capacitors. This subject is beyond the scope of this paper and will be the subject of future work.

References

[1] A. E. Ruehli, "Equivalent circuit models for three-dimensional multiconductor systems," *IEEE Trans. Microw. Theory Tech.*, vol. MTT-22, no. 3, pp. 216–221, Mar. 1974.

[2] A. E. Ruehli, "Circuit models for three-dimensional geometries including dielectrics," *IEEE Trans. Microw. Theory Tech.*, vol. 40, no. 7, pp. 1507–1516, Jul. 1992.

[3] M. N. Hu, J. Wang, and K.-L. Wu, "Enhanced PEEC modeling for embedded RF passives of irregular shapes," in *IEEE MTT-S Int. Microw. Symp. Dig.*, Jun. 2005, pp. 12–17.

[4] H. Shi, J. Fan, and J. Drewniak, "Modeling multilayered PCB power-bus designs using an MPIE based circuit extraction technique," in *Proc. IEEE EMC Int. Symp. Dig.*, Aug. 1998, pp. 647–651.

[5] A. M. Niknejad and R. G. Meyer, "Analysis, design, and optimization of spiral inductors and transformers for SI RF ICs," *IEEE J. Solid-State Circuits*, vol. 33, no. 10, pp. 1470–1481, Oct. 1998.

[6] G. Wollenberg and A. Gorisch, "Analysis of 3-D interconnect structures with PEEC using SPICE," *IEEE Trans. Electromagn. Compat.*, vol. 41, no. 4, pp. 412–417, Nov. 1999.

[7] J. Wang and K.-L. Wu, "A derived physically expressive circuit model for multilayer RF embedded passives," *IEEE Trans. Microw. Theory Tech.*, vol. 54, no. 5, pp. 1961–1968, May 2006.

[8] H. Hu, K. Yang, K.-L. Wu, and W. Y. Yin, "Quasi-static derived physically expressive circuit model for lossy integrated RF passives," *IEEE Trans. Microw. Theory Tech.*, vol. 56, no. 8, pp. 1954–1961, Aug. 2008.

[9] D. Gope, A. E. Ruehli, C. Y. Yang, and V. Jandhyala, "(S)PEEC: Time- and frequency-domain surface formulation for modeling conductors and dielectrics in combined circuit electromagnetic simulations," *IEEE Trans. Microw. Theory Tech.*, vol. 54, no. 6, pp. 2453–2464, Jun. 2006.

[10] G. Antonini, M. Sabatini, and G. Miscione, "PEEC modeling of linear magnetic materials," in *Proc. IEEE Electromag. Compat. Int. Symp. Dig.*, Aug. 2006, pp. 93–98.

[11] C.-S. Kim, J.-S. Park, D. Ahn, and J.-B. Lim, "A novel 1-D periodic defected ground structure for planar circuits," *IEEE Microw. Wireless Compon. Lett.*, vol. 10, no. 4, pp. 131–133, Apr. 2000.

[12] W.-T. Liu, C.-H. Tsai;, T.-W. Han, and T.-L. Wu, "An embedded common-mode suppression filter for GHz differential signals using periodic defected ground plane," *IEEE Microw. Wireless Compon. Lett.*, vol. 18, no. 4, pp. 248–250, Apr. 2008.

[13] D. M. Pozar, "A reciprocity method of analysis for printed slot and slot-coupled microstrip antennas," *IEEE Trans. Antennas Propag.*, vol. AP-34, no. 12, pp. 1439–1446, Dec. 1986.
[14] M. Kahrizi, T. K. Sarkar, and Z. A. Maricevic, "Analysis of a wide radiating slot in the ground plane of a microstrip line," *IEEE Trans. Microw. Theory Tech.*, vol. 41, no. 1, pp. 29–37, Jan. 1993.
[15] J. Sercu, N. Fache, F. Libbrecht, and P. Lagasse, "Mixed potential integral equation technique for hybrid microstrip-slotline multilayered circuits using a mixed rectangular-triangular mesh," *IEEE Trans. Microw. Theory Tech.*, vol. 43, no. 5, pp. 1162–1172, May 1995.
[16] R. C. Hall and R. Mosig, "The analysis of arbitrarily shaped aperture-coupled patch antennas via a mixed-potential integral equation," *IEEE Trans. Antennas Propag.*, vol. 44, no. 5, pp. 608–614, May 1996.
[17] K. A. Michalski and J. R. Mosig, "Multilayered media Green's functions in integral equation formulations," *IEEE Trans. Antennas Propag.*, vol. 45, no. 3, pp. 508–519, Mar. 1997.
[18] D. G. Fang, J. J. Yang, and B. Y. Delisie, "Discrete image theory for horizontal electric dipoles in a multilayered medium," *Proc. Inst. Elect. Eng.*, vol. 135, no. 5, pt. H, pp. 297–303, Oct. 1988.
[19] L. K. Yeung, "PEEC modeling of LTCC embedded RF passive devices," Mphil. thesis, Dept. Electron. Eng., Chinese Univ. Hong Kong, Shatin, Hong Kong, 2002, ch. 3.
[20] *IE3D User's Manual.*. Fremont, CA: Zeland Softw. Inc., 2002, Rel. 9.
[21] Advanced Design System (ADS). Agilent Technol., Santa Clara, CA, 2007. [Online]. Available: http://eesof.tm.agilent. com/products/ads_main.html
[22] N. Herscovici and D. M. Pozar, "Full-wave analysis of aperture-coupled microstrip lines," *IEEE Trans. Microw. Theory Tech.*, vol. 39, no. 7, pp. 1108–1114, Jul. 1991.

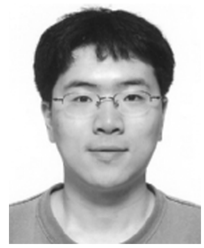

Kai Yang was born in Shanghai, China, in 1982. He received the B.Eng. and M.Eng. degrees in electronic engineering from Shanghai Jiao Tong University, Shanghai, China, in 2005 and 2008, respectively, and is currently working toward the Ph.D. degree at the University of Texas at Austin.

From 2005 to 2007, he was with the Center for Microwave and RF Technologies, Shanghai Jiao Tong University, Shanghai, China. Since March 2007, he has been with the Department of Electronic Engineering, The Chinese University of Hong Kong, Shatin, Hong Kong, as a Research Assistant. His current research interests include computational electromagnetics, the design of microwave components, and coupled EM/circuit simulation.

Ke-Li Wu (M'90–SM'96) received the B.S. and M.Eng. degrees from the Nanjing University of Science and Technology, Nanjing, China, in 1982 and 1985, respectively, and the Ph.D. degree from Laval University, Quebec, QC, Canada, in 1989.

From 1989 to 1993, he was with the Communications Research Laboratory, McMaster University, as a Research Engineer. In March 1993, he joined the Corporate Research and Development Division, Com Dev International, where he was a Principal Member of Technical Staff in charge of developing advanced EM design software for passive microwave subsystems for communication satellites. Since October 1999, he has been with the Department of Electronic Engineering, The Chinese University of Hong Kong, Shatin, Hong Kong, where he is currently a Professor. He has authored or coauthored numerous publications in the areas of EM modeling and microwave and antenna engineering. His current research interests include numerical and analytical methods in electromagnetics, passive microwave circuits, theory and practices of microwave filters, antennas for wireless terminals, low-temperature co-fired ceramic (LTCC) based multichip modules (MCMs) for wireless communications, and RF identification (RFID) technologies.